

Plasma Channel Formation and Guiding during High Intensity Short Pulse Laser Plasma Experiments

K. Krushelnick,² A. Ting,¹ C. I. Moore,¹ H. R. Burris,¹ E. Esarey,¹ P. Sprangle,¹ and M. Baine³

¹Plasma Physics Division, Naval Research Laboratory, Washington, D.C. 20375

²Laboratory of Plasma Studies, Cornell University, Ithaca, New York 14853

³University of California at San Diego, La Jolla, California 92093

(Received 19 July 1996)

A plasma channel is formed behind a self-guided, subpicosecond, 2 TW laser pulse in a hydrogen gas jet plasma. The channel is produced from the radial expulsion of plasma ions due to charge separation created in the displacement (or cavitation) of plasma electrons by the large ponderomotive force of the laser. Using Thomson scattering diagnostics and mode structure measurements, an intense trailing laser pulse ($I \sim 5 \times 10^{16}$ W/cm²) is observed to be guided throughout the length of this channel for about 20 Rayleigh lengths, approximately equal to the propagation length of the self-guided pump laser pulse. [S0031-9007(97)03234-1]

PACS numbers: 52.40.Nk, 42.65.Jx, 52.25.Rv, 52.70.Kz

The development of ultrahigh intensity lasers [1] over the past several years has led to a number of proposed applications—in particular, x-ray lasers [2], laser-driven electron accelerators [3], and the “fast ignitor” concept for inertial confinement fusion [4]. In practical terms, these applications require long laser propagation distances at high intensity in a plasma. This implies that the laser pulse must be “guided” for distances significantly greater than the vacuum diffraction length (Rayleigh range), which is typically less than a hundred microns if the beam is tightly focused. Guiding of intense laser pulses in preformed plasmas has been previously demonstrated by a variety of mechanisms. Laser light with intensities of up to 5×10^{15} W/cm² has been channeled up to 3 cm in a waveguide structure created by the hydrodynamic expansion of a preformed plasma [5], and intensities up to 10^{16} W/cm² have been guided using glass capillary waveguides in vacuum [6] and by using a plasma generated by a discharge [7].

In this paper, experiments at the Naval Research Laboratory (NRL) will be discussed in which we observe the creation of a plasma waveguide by a self-guided, high intensity ($I > 10^{18}$ W/cm²), short ($\tau \sim 0.4$ psec) laser pulse as it propagates in an underdense plasma. To investigate the evolution of the waveguide structure, an intense probe laser pulse ($\sim 5 \times 10^{16}$ W/cm²) is coupled into the plasma channel. In these experiments, the pump pulse is self-guided through self-modulation, relativistic self-focusing, and electron density displacement (cavitation) effects. For laser pulses above the critical power for relativistic optical guiding, given by $P_{\text{crit}} = 17 (\omega_0/\omega_{\text{pe}})^2$ GW (where ω_{pe} is the electron plasma frequency and ω_0 is the laser frequency), self-channeling of laser pulses in plasmas has been experimentally observed [8] and has been the subject of extensive theoretical examination [9]. Self-focusing of intense laser pulses in plasmas can also be enhanced by the expulsion of plasma electrons

(cavitation) produced by the extreme ponderomotive force of a focused laser pulse [10]. Subsequently, the radial electrostatic force from charge separation expels plasma ions from regions of electron density depletion in the focal volume of the high intensity pump pulse. Because of their inertia, the ions continue to drift radially outward even *after* the passage of the pump laser pulse and a plasma channel is formed. Our experiments show that a trailing laser pulse of relatively high intensity can be channeled in a structure produced by a 2 TW pump laser pulse for durations up to 50 psec after passage of the main beam. The propagation distance of the trailing beam is measured to be about 20 Rayleigh lengths. These phenomena may have particular relevance for the fast ignitor concept in laser fusion experiments.

These experiments were performed with the NRL tabletop terawatt laser system which operates at a wavelength of $1.054 \mu\text{m}$. The peak power is 2 TW with a typical pulse length of 400 fsec and a peak focused intensity of 6×10^{18} W/cm². The measured focal spot radius of $r_0 \sim 4.5 \mu\text{m}$ corresponds to a vacuum Rayleigh length of $Z_R = \pi r_0^2/\lambda \sim 60 \mu\text{m}$. To reduce effects of ionization induced defocusing [11], we used a gas jet of hydrogen (H_2) which produced a maximum plasma density of $n_e \approx 10^{19}$ cm⁻³ when ionized. The plasma has a uniform region of about 2 mm in the center of the jet and a density scale length of about 0.5 mm at the edges. A charge-coupled device (CCD) camera was positioned at 90° from the axis of laser propagation to image the interaction region, and a second CCD array was used to image the mode structure of the channeled pulse at the “exit” of the plasma channel.

The length of the interaction region was observed from images of the sidescattered Thomson emission ($\lambda_{\text{laser}} = 1054$ nm) from the pump light (*s* polarized) on the 90° CCD camera using an interference filter ($\Delta\lambda = 10$ nm). As the laser power was increased from 0.2 TW [Fig. 1(C)],

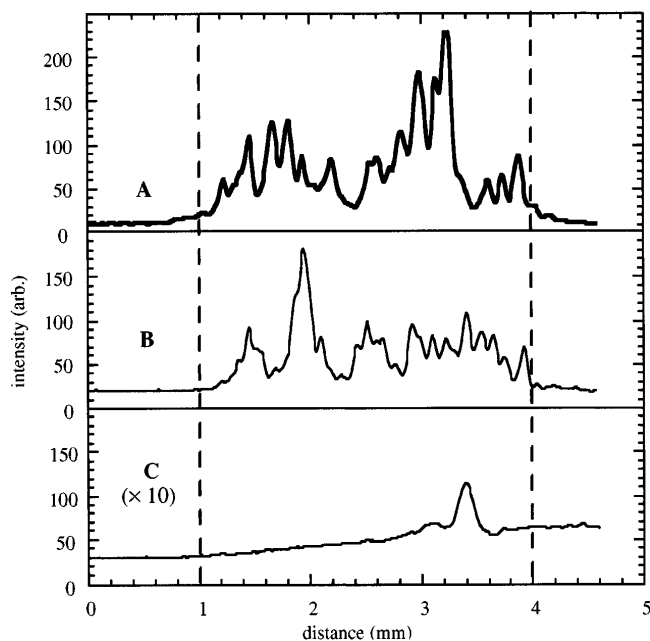


FIG. 1. Thomson scattered spatial profiles of the pump beam in a hydrogen gas jet for (A) 2 TW, (B) 1 TW, and (C) 0.2 TW. Dashed lines indicate the approximate extent of the gas jet. Laser propagation is from right to left.

the length of the emission region increased to about 2.5 mm at 2 TW [see Fig. 1(A)]. However, extended regions of self-focusing were observed for incident laser powers of about 1 TW [Fig. 1(B)] which is less than the theoretical critical power for relativistic self-focusing at these densities ($P_{\text{crit}} \sim 1.7$ TW). The width of these images was limited by the resolution of the imaging system ($< 100 \mu\text{m}$). Such guiding cannot be attributed to atomic nonlinear self-focusing effects since hydrogen gas is completely ionized at a relatively low intensity ($\sim 10^{14} \text{ W/cm}^2$). In addition, when preionizing pulses up to 10% of the total energy were used, no qualitative change in the Thomson scattered image from the interaction with the main pulse was observed. If we assume that the focal spot size of the laser pulse in the plasma is similar to that in vacuum, then this channeled region corresponds to a distance of greater than 40 Rayleigh lengths. The self-focusing of the pump laser is probably caused by self-modulation, relativistic self-focusing, and electron displacement which may lower the necessary power for self-guiding [12]. Images of the Thomson scattered light typically exhibited a number of separate foci in our experiments. The positions of these foci were not precisely reproducible from shot to shot and may have been due to envelope oscillations caused by a mismatch between defocusing diffraction effects and relativistic/electron displacement self-focusing effects.

A pump-probe experimental arrangement was used to monitor the temporal characteristics of the high intensity laser produced plasma. Approximately 10% of the main laser beam was reflected using a pellicle and subsequently

frequency doubled to 527 nm with a KD^*P crystal to form a probe beam. This intense probe pulse ($E \approx 10$ mJ, $\tau \approx 0.5$ psec) was then sent through an adjustable delay line and recombined with the main pulse before reaching the focusing optics (an off-axis parabolic mirror which focused the probe beam at $f/6$ and the pump beam at $f/3$). Temporal and spatial overlap of the two beams were achieved by monitoring the blueshift of the probe pulse wavelength and by imaging the interaction region [13]. The temporal resolution of our pump-probe measurements was better than 1 psec.

Thomson scattered emission from the probe-plasma interaction was imaged at 90° to the laser propagation direction onto a CCD through a 527 nm filter ($\Delta\lambda = 5$ nm). When only the probe pulse was injected into the gas jet, very little Thomson scattered emission was observed even though a plasma was created. However, if both pump and probe pulses were incident simultaneously on the gas jet, a bright image of scattered probe light (527 nm) was observed in the region where the pump beam was channeling. This emission is probably caused by coherent Thomson scattering of the probe laser from ion acoustic waves generated in the turbulent decay of the large amplitude plasma waves in the wake field of the pulse [13]. This scattered radiation was observed even as the temporal separation between the pump and probe laser pulses was increased by more than the laser pulse width (see Fig. 2). In fact, the brightness of the Thomson scattered image from the probe reached a maximum approximately 15 psec after passage of the pump pulse. Thomson scattered emission from the probe continued for pump-probe delays of more than 40 psec before decreasing significantly.

The image of Thomson side scattered radiation from the trailing probe beam (see Fig. 2) was observed to be qualitatively similar to the corresponding image of the pump beam, indicating that a waveguide structure is formed in the wake of the high intensity pump pulse. Although the pump pulse may be influenced by relativistic self-focusing, the probe pulse is too weak ($P_{\text{probe}} \sim 10^{-2} P_{\text{crit}}$) to impart relativistic quiver velocities to the plasma electrons. The plasma temperature from similar interactions has been measured immediately after the interaction to be about 100 eV [14], which results in a sound speed (C_s) of about $0.1 \mu\text{m/psec}$ and agrees with the time scales observed in the evolution of the Thomson scattered probe light. As the size of the plasma channel increases, the decrease in the probe light intensity contributes to the observed reduction in the level of Thomson emission. At large delays the observed emission near 527 nm [see Fig. 2(F)] is second harmonic light generated by the pump laser itself [15]. Identical experiments were performed in which helium was used as the target gas producing similar results, although the characteristic channel formation time was observed to be somewhat longer—consistent with the slower plasma sound speed [$\sim (m_{\text{H}}/m_{\text{He}})^{1/2}$].

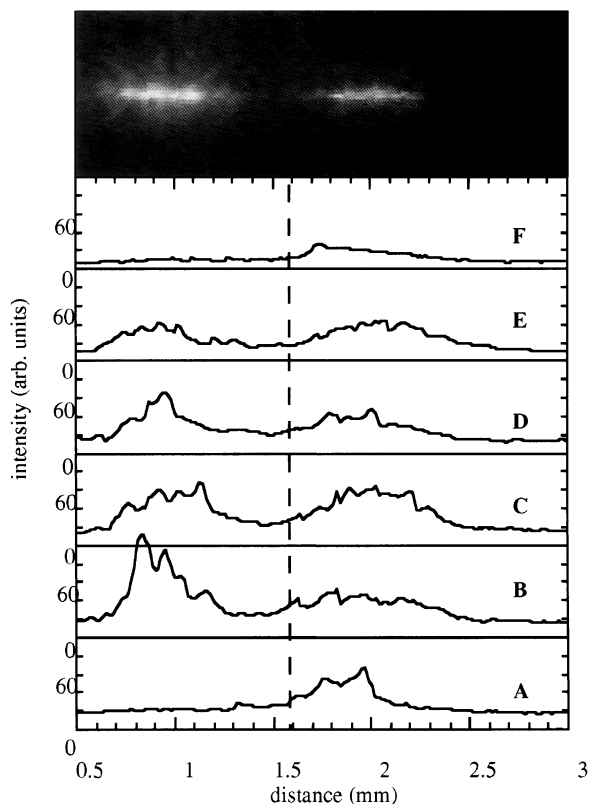


FIG. 2. Thomson scattered spatial profiles of probe beam (527 nm) for various delay settings between pump and probe in hydrogen gas jet: (A) 0, (B) 6, (C) 14, (D) 22, (E) 30, (F) 46 psec (propagation from right to left). Typical CCD image ($\Delta t = 19$ psec) shown at top. Dashed line indicates approximate position of vacuum focus (centered in gas jet).

We have also profiled the exit mode structure of the probe pulse during this interaction by imaging the focal spot with a microscope objective onto a CCD array. Such images were obtained by adjusting the axial position of the array so that the lens imaged the exit of the channel, as shown in Fig. 3. The waist of the central peak of the probe beam profile at the exit of the high intensity laser produced channel [Fig. 3(B)] is similar to the focal spot (radius $\sim 4.5 \mu\text{m}$) of the probe beam without plasma [Fig. 3(A)]. For Fig. 3(B) the channel exit was about 1.5 mm from the position of the vacuum best focus [Fig. 3(A)]. The exit mode from the channel essentially maintains the original single mode structure (radius $\sim 5 \mu\text{m}$) with surrounding diffraction rings and some lower intensity small scale structure. Without the focusing effect of the plasma waveguide the size of the probe beam is about $300 \mu\text{m}$ at this position. We have also measured the amount of light in the central lobe of the exit mode of channeled beam to be approximately $(75 \pm 15)\%$ of the input energy.

The formation of a plasma channel can be most easily attributed to the effects of ponderomotive forces associated with the intense pump laser pulse as it propagates through the plasma. Initially, the pump laser pulse exerts

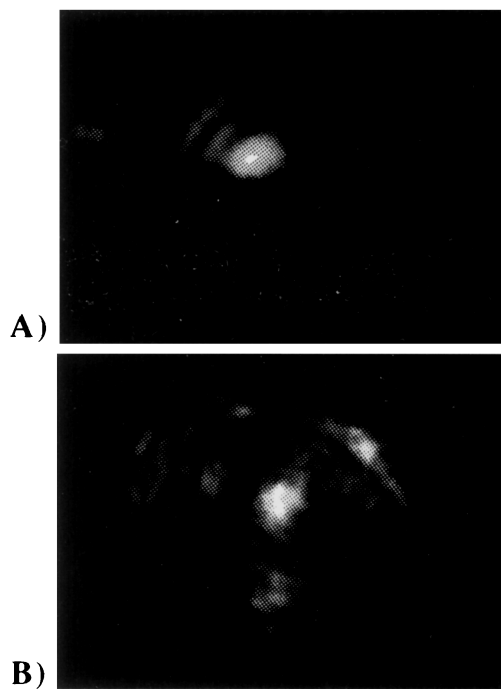


FIG. 3. (A) Image of probe beam vacuum focal spot ($1/e^2$ diameter $\sim 9 \mu\text{m}$). (B) Image of the guided probe beam waist at channel exit [scale is similar as in (A)].

a ponderomotive force on the plasma electrons and expels them radially. This sets up a large space charge force which propels the ions outward from the axis of propagation (a ‘‘Coulomb explosion’’ [2]). After the passage of the pump pulse, the ions continue to drift radially at approximately the ion acoustic speed $C_s = (ZT_e/m_i)^{1/2}$, thus creating a plasma channel, where Z is the number of electrons per ion, T_e (T_i) is the electron (ion) temperature, and m_e (m_i) is the electron (ion) mass. The electron motion is described by the radial force balance, $e\nabla_{\perp}\phi = m_e c^2 \nabla_{\perp}(1 + a^2/2)^{1/2} + n_e^{-1} \nabla_{\perp} P_e$, where $e\nabla_{\perp}\phi$ is the space charge force, $m_e c^2 \nabla_{\perp}(1 + a^2/2)^{1/2}$ is the ponderomotive force, $P_e = T_e n_e$ is the electron pressure, n_e is the electron density, and a^2 is related to the laser wavelength λ and intensity profile I by $a^2 = 7.2 \times 10^{-19} \lambda^2 [\mu\text{m}] I [\text{W}/\text{cm}^2]$. This expression neglects the generation of plasma waves and assumes that the axial length of the laser pulse is large compared to the laser spot size and the plasma wavelength. In the linear regime, the ion motion is described by the continuity equation $\partial \delta n_i / \partial t = -n_{i0} \nabla_{\perp} \cdot \mathbf{v}_{\perp}$ and the momentum equation $m_i \partial \delta \mathbf{v}_{\perp} / \partial t = -Z e \nabla_{\perp} \phi$, where δn_i and n_{i0} are the perturbed and ambient ion densities, \mathbf{v}_{\perp} is the radial ion velocity, and $T_i \ll T_e$ is assumed. Combining the electron radial force balance, the ion continuity equation, and the ion momentum equation yields

$$\left(\frac{\partial^2}{\partial t^2} - C_s^2 \nabla_{\perp}^2 \right) \frac{\delta n_i}{n_{i0}} \cong \frac{Z m_e}{4 m_i} \nabla_{\perp}^2 a^2, \quad (1)$$

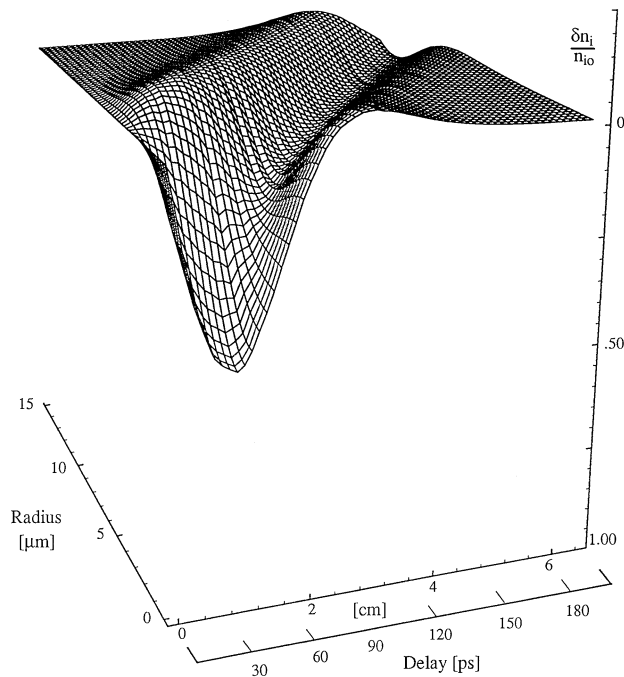


FIG. 4. Solution of Eq. (1) for parameters discussed in text.

assuming $\delta n_i^2/n_{i0}^2 \ll 1$, $a^2 \ll 1$, and an isothermal equation of state.

Using the 2D Green's function for the wave equation, the solution to Eq. (1) has been evaluated for a nonevolving laser pulse of the form $a^2 = a_0^2 f(\zeta) \exp(-2r^2/r_0^2)$, with $f = \sin^2(\pi\zeta/L)$ for $0 \leq \zeta \leq L$ and $f = 0$ otherwise, where $\zeta = z - ct$. The evolution of the density channel is shown in Fig. 4 for the illustrative parameters $a_0 = 0.25$, $r_0 = 10 \mu\text{m}$, $L = 120 \mu\text{m}$, $T_e = 100 \text{ eV}$, $Z = 2$, $m_i/m_e = 7300$, and $\beta_s = C_s/c = 2.3 \times 10^{-4}$. Figure 4 indicates a maximum density depletion ($\delta n_{i0}/n_{i0} \cong 0.47$) is reached at about 30 psec for the simulation parameters. Despite the simplifying assumptions used, these calculations clearly show that a short lived plasma channel can be created in the wake of a high intensity short pulse laser propagating through an underdense plasma—agreeing qualitatively with experimental results. It should also be noted that ponderomotive forces of the plasma wake field may also contribute to the formation and development of the channel [16]. The plasma temperature may also increase due to turbulent decay of these waves. However, such heating is probably a secondary

effect due to the long time scale required for thermal equilibration.

In conclusion, pump-probe laser experiments in underdense plasmas have been performed which demonstrate that a deep plasma channel ($\delta n_{i0}/n_{i0} \sim 1$) can be formed behind a very high intensity, self-guided ($40 Z_R$), pump pulse. An intense probe pulse ($\sim 5 \times 10^{16} \text{ W/cm}^2$) was guided over a distance approximately equal to the propagation distance of the pump pulse ($\sim 20 Z_R$). The temporal evolution of the channel was measured to have a duration of up to 50 ps in hydrogen plasmas, consistent with the model of channel formation due to ion displacement.

The authors would like to thank C. Manka, J. Grun, A. Fisher, J. Krall, and W. Leemans for useful discussions and L. Daniels and K. Evans for technical assistance. This work was supported by ONR and DOE.

-
- [1] M. D. Perry and G. Mourou, *Science* **264**, 927 (1994).
 - [2] N. H. Burnett and G. D. Enright, *IEEE J. Quant. Electron.* **26**, 1797 (1990).
 - [3] E. Esarey *et al.*, *IEEE Trans. Plasma Sci.* **24**, 252 (1996).
 - [4] M. Tabak *et al.*, *Phys. Plasmas* **1**, 1626 (1994).
 - [5] C. G. Durfee III and H. M. Milchberg, *Phys. Rev. Lett.* **71**, 2409 (1993); H. M. Milchberg *et al.*, *Phys. Plasmas* **3**, 2149 (1996).
 - [6] S. Jackel *et al.*, *Opt. Lett.* **20**, 1086 (1995).
 - [7] Y. Ehrlich *et al.*, *Phys. Rev. Lett.* **77**, 4186 (1996).
 - [8] A. B. Borisov *et al.*, *Phys. Rev. Lett.* **68**, 2309 (1992); A. Sullivan *et al.*, *Opt. Lett.* **19**, 1544 (1994); P. Monot *et al.*, *Phys. Rev. Lett.* **74**, 2953 (1995).
 - [9] P. Sprangle *et al.*, *Phys. Rev. Lett.* **69**, 2200 (1992); K. C. Tzeng *et al.*, *Phys. Rev. Lett.* **76**, 332 (1996).
 - [10] G. Z. Sun *et al.*, *Phys. Fluids* **30**, 526 (1987); W. B. Mori *et al.*, *Phys. Rev. Lett.* **60**, 1298 (1988); P. Sprangle *et al.*, *Appl. Phys. Lett.* **58**, 346 (1991); K. Krushelnick *et al.*, *Phys. Rev. Lett.* **75**, 3681 (1995).
 - [11] W. P. Leemans *et al.*, *Phys. Rev. A* **46**, 1091 (1992); P. Monot *et al.*, *J. Opt. Soc. Am. B* **9**, 1579 (1992).
 - [12] E. Esarey *et al.*, *Phys. Rev. Lett.* **72**, 2887 (1994); A. Chiron *et al.*, *Phys. Plasmas* **3**, 1373 (1996).
 - [13] A. Ting *et al.*, *Phys. Rev. Lett.* **77**, 5377 (1996).
 - [14] T. E. Glover *et al.*, *Phys. Rev. Lett.* **73**, 78 (1994); W. J. Blyth *et al.*, *Phys. Rev. Lett.* **74**, 554 (1995).
 - [15] J. A. Stamper *et al.*, *Phys. Fluids* **28**, 2563 (1985); P. E. Young *et al.*, *Phys. Rev. Lett.* **63**, 2812 (1989); A. Ting *et al.*, *Opt. Lett.* **21**, 1096 (1996).
 - [16] W. Mori (private communication).